Original Research

In vitro enzyme-mimic activity and *in vivo* therapeutic potential of HSJ-0017, a novel Mn porphyrin-based antioxidant enzyme mimic

Bao-qiu Li[1], Xin Dong[2], Na Li[2], Ji-you Gao[2], Qiang Yuan[2], Shi-hong Fang[2], Xian-chang Gong[3], Shu-juan Wang[4] and Feng-shan Wang[1]

[1]School of Pharmaceutical Sciences, Shandong University, Jinan, Shandong 250012, China; [2]Shandong Hongli Laboratory Animal Experiment Co, Ltd, Jinan, Shandong 250101, China; [3]Jinan Saiwen Pharmaceuticals, Inc, Jinan, Shandong 250101, China; [4]Jilin Province A-Think Pharmaceutical Co, Ltd, Changchun, Jilin 130616, China
Corresponding author: Feng-shan Wang. Email: wangfengshanda@126.com

Abstract

Manganese (III) 5, 10, 15, 20-tetrakis [3-(2-(2-methoxy)-ethoxy) ethoxy] phenyl porphyrin chloride, designated HSJ-0017, is a novel antioxidant enzyme mimic. The aim of the present study was to investigate the enzyme-mimic activity and the therapeutic potential of HSJ-0017 in free radical-related diseases. Superoxide dismutase (SOD) mimic activity was measured by the nitroblue tetrazolium chloride monohydrate reduction assay. Catalase (CAT) mimic activity was measured based on the decomposition of hydrogen peroxide. The antitumor, radioprotective and chemoprotective effects of HSJ-0017 were evaluated in H22 or S180 tumor-bearing Kunming mice. The anti-inflammatory and hepatoprotective effects were, respectively, evaluated in histamine-induced edema model and CCl_4-induced hepatic damage model in Wistar rats. HSJ-0017 over a concentration range of 0.001–10 μmol/L significantly inhibited the generation of superoxide anion. Significant hydrogen peroxide scavenging activity was observed when the concentration of HSJ-0017 was higher than 0.01 μmol/L. HSJ-0017 at a dose of 3.0 mg/kg exhibited significant antitumor effect on S180 tumor xenografts, whereas no significant antitumor effect was observed in H22 tumor xenografts. HSJ-0017 at a dose of 3.0 mg/kg enhanced the antitumor effects of radiotherapy and chemotherapy, and reduced their toxicity. However, HSJ-0017 counteracted the antitumor effects of radiotherapy when administered simultaneously with radiotherapy. HSJ-0017 showed significant anti-inflammatory and hepatoprotective effects. Our results demonstrate that HSJ-0017 exhibits antioxidant, antitumor, anti-inflammatory, radioprotective, chemoprotective, and hepatoprotective effects. It is a potent dual SOD/CAT mimic.

Keywords: Mn-porphyrins, antioxidant, superoxide dismutase, free radical, radioprotection

***Experimental Biology and Medicine* 2014; 239: 1366–1379. DOI: 10.1177/1535370214532598**

Introduction

Free radicals are reactive chemical species that contain one or more unpaired electrons. High levels of free radicals, such as superoxide anion (O_2^-), hydrogen peroxide (H_2O_2), and hydroxyl radical (·OH), have been detected in several human cell lines as well as in different human tissues. Although physiological levels of free radicals are necessary for the maturation process of cellular structures and high levels of free radicals can be produced by radiation and some chemotherapy agents to kill rapidly dividing cancer cells,[1] extensive evidence has been accumulated which shows that these reactive species mainly produced in the mitochondria via the electron transport chain play important roles in many human diseases and pathophysiological processes (e.g. inflammation, ischemia-reperfusion injury, and cancer).[2–4] Moreover, free radical-mediated processes are also implicated in radiotherapy- and chemotherapy-induced toxicities.[5,6] It is widespreadly believed, therefore, that antioxidant therapy, especially targeting antioxidants to mitochondria, is a promising new therapeutic strategy in the wide range of free radical-related diseases.[7]

Superoxide dismutase (SOD), catalase (CAT), and glutathione peroxidase (GPx), which contain redox-active metal centers and are therefore able to catalytically scavenge particular kind of free radicals at a high rate without interacting with other free radicals, are the primary antioxidant enzymes present in mammalian cells. These antioxidant enzymes exhibit promising potential for the treatment of free radical-related diseases with selective and superior antioxidant properties.[8–12] The native antioxidant enzymes, however, suffer from several drawbacks as potential drug

candidates. In light of the clinical data surrounding the use of antioxidant enzymes, low molecular weight catalytic mimics of antioxidant enzymes have been proposed for the treatment of a wide variety of diseases.[11,13] These mimics could have distinct advantages over the natural enzymes as pharmaceutical agents, including high stability, long half-life, improved cellular permeability, and low immunogenicity.

Over the past few decades, low molecular weight antioxidant enzyme mimics have been widely researched. Among them, Mn-porphyrins have shown promising antioxidant properties against cancers, inflammation, asthma, radiation injury, bleomycin-induced pulmonary fibrosis, and amyotrophic lateral sclerosis with SOD and CAT activities, and are thought being safe.[14,15] However, most Mn-porphyrins display poor liposolubility which limits the cumulative amount in the cells, whereas lipophilic Mn-porphyrins have been reported to exert considerable toxicity even at low dose.[16] Hence, there still remains a need to develop antioxidant enzyme mimics with superb potency, high lipophilicity, and low toxicity.

Manganese (III) 5, 10, 15, 20-tetrakis [3-(2-(2-methoxy)-ethoxy) ethoxy] phenyl porphyrin chloride (molecular formula: $C_{64}H_{68}ClMnN_4O_{12}$; molecular weight: 1174.39, Figure 1), designated HSJ-0017, is one of the lipophilic Mn porphyrin-based mimics of antioxidant enzymes developed by our group for the treatment of free radical-related diseases. Our previous studies have demonstrated that HSJ-0017 can be rapidly distributed to blood-rich organs and accumulated in mitochondria after intravenous injection.[17] Preliminary pharmacological studies have revealed that HSJ-0017 can enhance the therapeutic effects and reduce the toxicities of radiation and cyclophosphamide in B16/F1 murine melanoma-bearing C57BL/6 mice.[18]

Despite its good pharmacokinetic properties and potent, synergistic antitumor effects, the therapeutic potential of HSJ-0017 has not been extensively studied. Recent studies indicate that radiotherapy and some chemotherapeutic agents act by producing free radicals.[1] The radioprotective and chemoprotective effects of antioxidants may be influenced by the timing of drug administration.[19,20] Therefore, the purposes of the present study were to: (1) determine the *in vitro* enzyme-mimic activity of HSJ-0017, (2) investigate the *in vivo* therapeutic potential of HSJ-0017 in free radical-related diseases, such as cancers, inflammation, and CCl_4-induced hepatic damage in order to select appropriate indications for HSJ-0017, and (3) investigate the effect of timing of HSJ-0017 administration (e.g. pre-radiation, during radiation, and post-radiation) on its radioprotective and chemoprotective effects. To the best of our knowledge, limited experimental data have hitherto been available with regards to the relationship between the timing of Mn porphyrins administration and their radioprotective/chemoprotective effects.

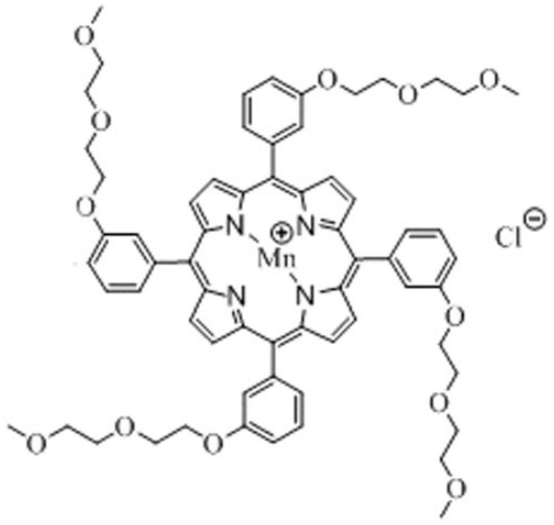

Figure 1 Structures of HSJ-0017

Materials and methods

Chemicals and reagents

Normal saline (NS, 0.9% NaCl) was obtained from Shandong Qidu Pharmaceutical Co. Ltd. (Shandong, Zibo, China). Carboplatin (CB) was provided by Shandong Qilu Pharmaceutical Co., Ltd. (Shandong, Jinan, China). Bovine Cu/Zn SOD, bovine liver CAT, butylated hydroxytoluene (BHT), desferrioxamine (iron chelator), dexamethasone, *N*,*N*-dimethyl formamide (DMF), ethylenediaminetetraacetic acid (EDTA), (−)epinephrine, glutathione, glutathione reductase, glycine, histamine, H_2O_2, NADPH, nitroblue tetrazolium chloride monohydrate (NBT), sodium phosphate, sodium azide, pentobarbital sodium, xanthine, and xanthine oxidase were purchased from Sigma-Aldrich Chemical Co. (St. Louis, MO). CCl_4 was purchased from Damao Chemical Reagent Factory (Tianjin, China). Olive oil was bought from Shanghai Kerry Food Industries Co., Ltd. (Shanghai, China).

Cell lines and culture

Murine H22 hepatoma cells (H22) and mouse sarcoma 180 cells (S180), purchased from Shanghai Institutes for Biological Sciences of Chinese Academy of Sciences (Shanghai, China), were cultured in RPMI-1640 medium (Gibco, Gran Island, NY) supplemented with 10% heat-inactivated fetal bovine serum (Gibco), 100 U/mL penicillin, and 100 μg/mL streptomycin at 37°C in 5% CO_2 incubator. The cells were subcultured until reaching the logarithmic growth phase.

Animals

Healthy specific pathogen-free Kunming mice (KM, male, 23–28 g, Certificate No.: SCXK2008-0002) and Wistar rats (male, 120–150 g, Certificate No.: SCXK2013-0001) were purchased from Shandong Lukang Pharmaceutical Group Co., Ltd. (Shandong, Jinan, China) and acclimatized at a temperature of 24 ± 4°C and a relative humidity of 50 ± 5% under 12 h day/night cycle for one week prior to treatment. Animals were allowed free access to food and water. All experimental procedures involving animals were conducted in accordance with the International Guiding

Principles for Biomedical Research Involving Animals (2011), and approval has been received from our institutional animal ethics committee.

Preparation of HSJ-0017

HSJ-0017 was synthesized in four steps (Figure 2) and characterized in our lab. All reagents, including chemicals and solvents, were commercial products of reagent-grade quality purchased from Sigma-Aldrich Chemical Co.. For *in vitro* experiments, HSJ-0017 was dissolved in DMF. For *in vivo* administration, HSJ-0017 was dissolved in NS containing 1% DMF.

Compound 1: Methylene chloride (2 L), triethylamine (230 g), and 2-(2-methoxyethoxy) ethanol (225 g) were mixed in a three-necked flask. The solution was cooled below 0°C, and *p*-toluenesulfonyl chloride (358 g) was added dropwise. The temperature was not allowed to exceed 0°C. After the addition of *p*-toluenesulfonyl chloride was complete, the mixture was stirred overnight, and was monitored by thin layer chromatography (TLC) (Silica Gel. EtOAc/Hex 1:4). Upon completion, the solution was diluted with distilled water (2 L) and was washed with saturated sodium bicarbonate solution (1 × 1 L) followed by brine (2 × 1 L). The organic layer was dried over anhydrous sodium sulfate, and the solvent was removed under reduced pressure. The crude product was purified by using column chromatography on Silica Gel (EtOAc/Hex 1:4) to give **compound 1** (429 g, 83.5%).

Compound 2: Compound 1 (292 g) was dissolved in dimethylformamide (1.3 L). Anhydrous K_2CO_3 (450 g) and *m*-hydroxybenzaldehyde (132 g) were then added. The mixture was heated to 80°C for 3 h, and was monitored by TLC (Silica Gel. EtOAc/Hex 1:2). Upon completion, the solvent was evaporated *in vacuo* and the residue was dissolved in distilled water (1 L). After filtration, the solution was extracted three times with methylene chloride. The combined extracts were washed with brine, dried over anhydrous sodium sulfate, and concentrated *in vacuo*. The crude product was purified by using column chromatography on Silica Gel (EtOAc/Hex 1:2) to give **compound 2** (248 g, 103.9%).

Ms (ESI): m/z 225.4 ($M+H^+$), 242.4 ($M+NH_4^+$), 247.3 ($M+Na^+$).

^{1}H-NMR ($CDCl_3$, 600 MHz) σ: 9.975 (s, 1H, –CHO), 7.480–7.414 (m, 2H), 7.227–7.214 (d, 2H, $J=7.74$ Hz), 4.220–4.216 (m, 2H, $-CH_2-$), 3.904–3.901 (m, 2H, $-CH_2-$), 3.745–3.741 (m, 2H, $-CH_2-$), 3.601–3.593 (m, 2H, $-CH_2-$), 3.407 (s, 3H, $-OCH_3$).

^{13}C-NMR($CDCl_3$, 600 MHz) σ: 192.510, 159.378, 137.739, 130.075, 123.647, 122.077, 112.965, 71.933, 70.798, 69.626, 67.664, 59.119.

Compound 3: A solution of pyrrole (67 g) in propionic acid (0.5 L) was added dropwise to a propionic acid solution (0.3 L) of compound 2 (224 g) under magnetic stirring within 6 h. The mixture was stirred at 125°C for three days, and was monitored by TLC (Silica Gel. Methylene chloride). Upon completion, the mixture was cooled to room

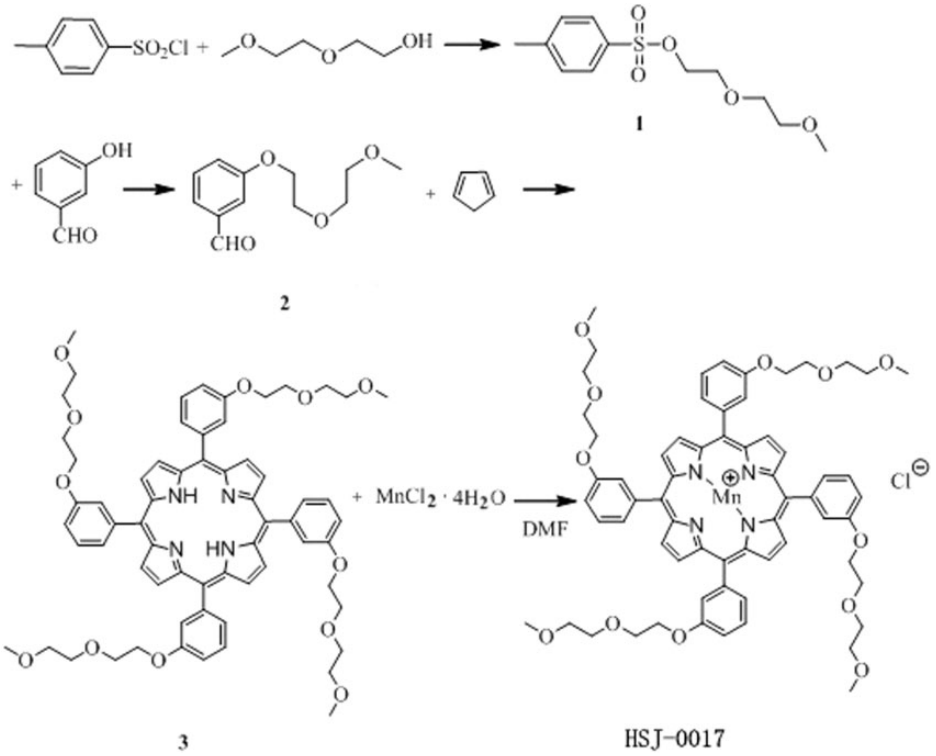

Figure 2 Synthesis scheme of HSJ-0017. Further details are described in ''Materials and methods'' section

temperature and the suspension was filtered. The filter cake was washed with propionic acid (1 L), and concentrated *in vacuo*. The crude product was purified by using column chromatography on silica gel (methylene chloride) to give **compound 3** (48 g, 4.42%).

Ms (ESI): m/z 1087.9 ($M + H^+$).

^{1}H-NMR ($CDCl_3$, 600 MHz) σ: 8.928 (s, 8H, –pyrrol), 7.866–7.368 (m, 16H, Ar–H), 4.361 (2H, $-CH_2-$), 3.958 (2H, $-CH_2-$), 3.768 (2H, $-CH_2-$), 3.602 (2H, $-CH_2-$), 3.395 (3H, $-OCH_3$), –2.770 (s, 2H, NH).

^{13}C-NMR ($CDCl_3$, 600 MHz) σ: 157.22, 143.45, 127.93, 127.57, 121.22, 119.90, 114.27, 71.98, 70.84, 69.92, 67.68, 59.14.

HSJ-0017: Compound 3 (42 g), manganese (II) chloride tetrahydrate (53.6 g) and dimethylformamide (0.5 L) were mixed in a three-necked flask. The solution was heated under reflux for 7 h. After solvent evaporation, the residue was dissolved in methylene chloride (500 mL) and filtered. The filter cake was washed with methylene chloride (100 mL) and concentrated *in vacuo*. The crude product was purified by using column chromatography on silica gel (DCM/MetOH 95:5) to give **HSJ-0017** (42 g, 95.4%).

Ms (ESI): m/z 1139.8 (M^+).

^{1}H-NMR ($CDCl_3$, 600 MHz) σ: 8.24 (6H), 7.28–7.02 (3H), 4.38–3.52 (44H).

^{13}C-NMR ($CDCl_3$, 600 MHz) σ: 163.87, 132.19, 117.50, 116.46, 109.04, 108.31, 104.60, 72.27, 71.07–70.08, 67.98, 59.70–59.54, 54.78.

In vitro antioxidant enzyme-mimic activities of HSJ-0017

SOD mimic activity was measured by the NBT reduction method using xanthine plus xanthine oxidase as the O_2^--generating system and bovine Cu/Zn SOD as the standard. Prior to performing the study, we examined whether the metal complex inhibited the O_2^--generating system by monitoring uric acid formation spectrophotometrically at 295 nm.[21] A DMF solution containing a mixture of HSJ-0017 and NBT was prepared and incubated at 25°C to examine whether the metal complex reacts independently with NBT. The concentration of NBT in the solution was determined according to the method of Berkó and Schneider.[22]

The assay mixture contained 50 mmol/L sodium phosphate (pH 7.8), 250 μmol/L xanthine, 17.7 mU mL^{-1} xanthine oxidase, 2750 U mL^{-1} CAT, 10 μmol/L NBT, and various concentrations of HSJ-0017 (0.001, 0.01, 0.1, 1.0, and 10 μmol/L). Reduction of NBT into formazan complex was followed at 550 nm with a Shimadzu UV160A UV/VIS spectrophotometer (Shimadzu, Chiyoda-ku, Tokyo, Japan) after the addition of xanthine oxidase and thermostated at 25°C. A control reaction was carried out without HSJ-0017. The % inhibition of NBT reduction was calculated according to the following equation: % inhibition $= (A_0 - A_t/A_0) \times 100$; where A_0 was the absorbance of the control (without HSJ-0017) and A_t was the absorbance in the presence of HSJ-0017. The IC_{50} value (concentration required to inhibit NBT reduction by 50%) was obtained by linear regression analysis.

CAT mimic activity was assayed spectrophotometrically following the method proposed by Beers and Sizer.[23,24] The assay mixture contained 50 mmol/L sodium phosphate (pH 7.0) 10 mmol/L H_2O_2, and various concentrations of HSJ-0017 (0.001, 0.01, 0.1, 1.0 and 10 μmol/L). Decomposition of H_2O_2 was monitored with a Shimadzu UV160A UV/VIS spectrophotometer (Shimadzu) at 240 nm for 5 min at 25°C against a blank containing all the ingredients without the test samples. The H_2O_2 scavenging activity of HSJ-0017 was calculated according to the following equation: H_2O_2 scavenging activity (%) $= (A_0 - A_t/A_0) \times 100$; where A_0 was the absorbance of the control (without HSJ-0017) and A_t was the absorbance in the presence of HSJ-0017.

DMF concentrations in the assay never exceeded 1%.[23] The range of concentrations selected for HSJ-0017 was based on its solubility in water (13.6 μmol/L) and the IC_{50} of Cu/Zn SOD (0.0011 μmol/L).[25]

In vivo antitumor and radioprotective effects of HSJ-0017 in H22 tumor-bearing mice

H22 cells were injected intraperitoneally into eight male KM mice. After passage *in vivo* for seven days, H22 cells with ascites were harvested, diluted to a concentration of 2.5×10^7 cells/mL with sterilized NS, and inoculated subcutaneously into the right armpit region of male KM mice (5.0×10^6 cells/mouse). Tumor diameters were measured every other day with a vernier caliper and then converted to tumor volume (V) using the equation: $V = ab^2/2$, where a is the largest superficial diameter and b is the smallest superficial diameter. When the tumors reached a size of 100–150 mm^3, the tumor-bearing mice were randomly divided into six groups (10 mice/group) and treated as follows: group 1 (vehicle control) received NS containing 1% DMF, group 2 received 3.0 mg/kg HSJ-0017, group 3 received a single total body irradiation (TBI) of 7.0 Gy, group 4 received 3.0 mg/kg HSJ-0017 followed 2 h later by 7.0 Gy TBI, group 5 received 7.0 Gy TBI followed 2 h later by 3.0 mg/kg HSJ-0017 and group 6 received 3.0 mg/kg HSJ-0017 immediately after 7.0 Gy TBI. Both vehicles and HSJ-0017 were given by intravenous injection. Blood samples were collected from the retro-orbital venous plexus before treatment (day 0) and on days 3, 7, and 10 post treatment. Hematological indices, including white blood cell (WBC, $\times 10^9$/mL) count, red blood cell (RBC, $\times 10^{12}$/mL) count, and platelet (PLT, $\times 10^{12}$/mL) count were analyzed with a BC2200 Automatic Hematology Analyzer (Shenzhen Mindray Bio-Medical Electronics Co, Ltd., Guangdong, Shenzhen, China). Tumor diameters were measured before treatment (day 0) and on day 10 post treatment. The inhibition rate of tumor growth was calculated according to the following formula: tumor inhibitory rate (%) = (1 −[ending average tumor volume of treatment group – starting average tumor volume of treatment group]/[ending average tumor volume of vehicle control group – starting average tumor volume of vehicle control group]) × 100%.

In our previous studies, different doses of HSJ-0017 (0.3, 1.0 and 3.0 mg/kg) exhibited significant antitumor, chemoprotective, and radioprotective effects in B16/F1 tumor-bearing animals, and did not elicit any toxic symptoms in animals.[18] The highest dose (3.0 mg/kg) was used in the

present study. The dosage schedule selected for HSJ-0017 was based on the data from our pharmacokinetic studies[17] and other pilot studies (unpublished data).

In vivo antitumor and chemoprotective effects of HSJ-0017 in S180 tumor-bearing mice

S180 solid tumor model was also established by subcutaneous injection. Briefly, S180 cells were passaged twice in the abdominal cavity of male KM mice. After *in vivo* passages, the seroperitoneum was extracted with a sterilized syringe, conventionally prepared, and then inoculated subcutaneously into the right armpit region of male KM mice (2.0×10^6 cells/mouse). When the tumors reached a size of 100–150 mm^3, the tumor-bearing mice were randomly divided into six groups (10 mice/group) and treated as follows: group 1 (vehicle control group) received NS containing 1% DMF, group 2 received 3.0 mg/kg HSJ-0017, group 3 received 30 mg/kg CB, group 4 received 3.0 mg/kg HSJ-0017 followed 2 h later by 30 mg/kg CB, group 5 received 30 mg/kg CB followed 8 h later by 3.0 mg/kg HSJ-0017, and group 6 received 30 mg/kg CB concurrent with 3.0 mg/kg HSJ-0017. All reagents including vehicles, HSJ-0017, and CB were given by intravenous injection. Tumor diameters and body weight were measured before treatment (day 0) and on days 1, 4, and 8 post treatment. The inhibition rate of tumor growth was estimated according to the formula above.

All tumor-bearing mice were sacrificed on the 8th day. Spleen and thymus were weighed immediately. The thymus index and spleen index were calculated according to the following equation: Thymus or spleen index (mg/g) = (average thymus weight or spleen weight/average body weight) × 100%. The selection of HSJ-0017 dosage was based on our previous study.[18] The dosage schedule selected for HSJ-0017 was based on the pharmacokinetic data of HSJ-0017 and CB.[17,26]

In vivo anti-inflammatory effects of HSJ-0017

Histamine-induced paw edema was used as the animal model of acute inflammation according to the method of Hira *et al*.[27] Paw edema was induced by subplantar injection of 0.1 mL of 0.1% freshly prepared solution of histamine into the right hind paw of Wistar rats. Animals were randomly distributed into five groups ($n = 10$) and treated as follows, 1 h before eliciting paw edema: group 1 (vehicle control) received NS containing 1% DMF, group 2 (positive control) received 1 mg/kg dexamethasone,[28] and the other three experimental groups received different doses of HSJ-0017 (0.3, 1.0 and 3.0 mg/kg), respectively. All reagents including vehicles, HSJ-0017, and dexamethasone were given by intraperitoneal injection. The paw volume was measured at 2 h before and 1, 2, 4, 6, 8, and 10 h after histamine injection using Ugo Basile Plethysmometer N 7140 (UGO Basile, Comerio, Italy). Percent change in edema volume was calculated according to the following equation: Percent change in edema volume (%) = $(V_t - V_0)/V_0 \times 100\%$, where V_0 (mL) was the average paw volume before injection and V_t (mL) was the average paw volume after injection.

In vivo hepatoprotective effects of HSJ-0017 on CCl_4-induced damage in rat

A rat model of CCl_4-induced hepatic damage was established following the method proposed by Sikander *et al.*,[29] with slight modifications. Male Wistar rats were randomized into five groups ($n = 10$). Group 1 served as a normal control group and received olive oil only. Groups 2–5 received intraperitoneal administration of CCl_4 2.0 mL/kg (40% CCl_4 in olive oil) twice a week for two weeks to induce hepatic damage followed by half the initial dose of CCl_4 twice a week for two weeks so as to maintain hepatic damage. Starting on the first day of CCl_4 administration, rats in groups 2–5 were treated with NS containing 1% DMF (model control) or different doses of HSJ-0017 (0.3, 1.0 and 3.0 mg/kg) once daily intravenously for 28 consecutive days.

At the end of the experiment, the rats were anesthetized by inhalation of diethyl ether, and blood samples were collected from the retro-orbital venous plexus. Serum was separated by centrifugation at $4000 \times g$ for 10 min. Serum biochemical parameters including alanine transaminase (ALT, IU/L), aspartate transaminase (AST, IU/L), alkaline phosphatase (ALP, IU/L), lactate dehydrogenase (LDH, IU/L), and gamma glutamyltransferase (GGT, IU/L) were detected using a Mindray BA-90 biochemical analyzer (Mindray Medical International Ltd., Shenzhen, China).

All rats were sacrificed after blood collection. Liver tissues were excised, postfixed with 10% neutral buffered formalin, dehydrated in graded alcohol, embedded in paraffin, sectioned (5 μm), and stained with hematoxylin and eosin (H-E). The sections were examined histopathologically using an Olympus IX70 microscope (Olympus Optical Co., Tokyo, Japan).

For antioxidant enzyme assays, liver tissues from different groups were perfused with ice-cold NS and homogenized in 50 mmol.L sodium phosphate buffer (pH 7.4) containing 2 mmol/L EDTA, 0.13 mmol/L BHT, and 0.13 mmol/L desferrioxamine. The homogenate was centrifuged at $800 \times g$ to remove cellular debris. The supernatant was centrifuged at $10{,}000 \times g$ for 20 min at 4°C to get the post-mitochondrial supernatant (PMS). Hepatic SOD, CAT, and GPx activities were measured according to previously described methods.[29,30]

Briefly, SOD activity was assayed in a reaction mixture consisted of 0.8 mL of 50 mmol/L glycine buffer (pH 10.4) 0.02 mL of 20 mg/mL solution of (−) epinephrine, and 0.2 mL PMS. Oxidation of (−) epinephrine was monitored at 480 nm at 25°C. SOD activity was expressed as the enzyme required for 50% inhibition of (−) epinephrine autoxidation. CAT activity was assayed in a reaction mixture (3.0 mL) consisting of 0.05 mol/L sodium phosphate buffer (pH 7.0), 0.019 mol/L H_2O_2, and 0.05 mL PMS. Decomposition of H_2O_2 was monitored at 240 nm at 25°C. CAT activity was expressed as U/mg of protein. GPx activity was assayed in a reaction mixture (2.0 mL) consisted of 0.2 mmol/L H_2O_2, 1 mmol/L glutathione, 1.43 mmol/L NADPH, 1 mmol/L sodium azide, 0.1 mol/L sodium phosphate buffer (pH 7.0), 1.4 unit of glutathione reductase, and 0.1 mL PMS. The conversion of NADPH to $NADP^+$ was recorded at 340 nm. GPx activity was

expressed as μmoles of NADPH oxidized to $NADP^+$ min^{-1} mg^{-1} protein.

Statistics analysis

Data were calculated by SPSS17.0. Values were expressed as mean ± standard deviation (SD). Statistical analysis was performed by one-way analysis of variance (ANOVA) followed by Dunnett's multiple comparison test.

Results

Preparation and *in vitro* enzyme-mimic activities of HSJ-0017

HSJ-0017 was obtained as a dark green solid. The ^1H NMR and ^{13}C NMR spectra of HSJ-0017 are presented in Figure 3a and b, respectively. As various Mn-porphyrins which are commonly regarded as SOD mimics have been demonstrated to possess dual enzymatic activity,[31] we tested HSJ-0017 for its SOD- and CAT-mimic activities.

Cytochrome c- and NBT-reduction assays are the most frequently used indirect assays to detect the generation of O_2^- in an enzymic reaction system.[32] Although cytochrome C is the most specific O_2^- indicator and commonly used to study the kinetics of SOD mimics, it is less sensitive than NBT and often generates artifacts in the SOD activity assay of Mn-porphyrins.[25,33,34] Thus, NBT-reduction assay was used to determine the SOD mimic activity of HSJ-0017 in the present study. To rule out the possibility that HSJ-0017 may interact with xanthine oxidase and NBT, we measured the formation of uric acid in assay mixtures and determined the concentration of NBT in a control mixture. No significant change in absorbance was observed at 295 nm for HSJ-0017 at the range of concentrations used in the present study. No reaction was observed between HSJ-0017 and NBT. Therefore, the reduction in the generation of formazan complex can be ascribed to the O_2^- scavenging activity of HSJ-0017.

As shown in Figure 4a, HSJ-0017 over a concentration range of 0.001–10 μmol/L significantly inhibited the generation of O_2^- in a dose-dependent manner. At the concentration of 10 μmol/L, HSJ-0017 caused 89.07 ± 19.08% inhibition of O_2^- generation. Under these conditions, IC_{50} concentrations for the inhibition of NBT reduction by HSJ-0017 and bovine Cu/Zn SOD were found to be 0.0218 μmol/L (95% confidence interval: 0.0193–0.0307 μmol/L) and 0.0011 μmol/L (95% confidence interval: 0.0006–0.0024 μmol/L), respectively. In other words, HSJ-0017 was about 20-fold less active than bovine Cu/Zn SOD. The IC_{50} concentration for bovine Cu/Zn SOD obtained in the present study was consistent with previous reports.[25] The CAT mimic activity of HSJ-0017 is shown in Figure 4b. No significant H_2O_2 scavenging activity was observed when the concentration of HSJ-0017 was lower than 0.01 μmol/L, despite a slight reduction at the concentration of 0.01 μmol/L. In reaction mixtures containing high concentrations of HSJ-0017 (0.1–10 μmol/L), the amount of H_2O_2 detected fell from 12.87 ± 10.1% to 52.30 ± 21.84% of the control value within 5 min after being exposed to HSJ-0017, suggesting that high concentrations of HSJ-0017 are capable of quickly scavenging H_2O_2. These results obtained from enzyme-mimic activity assays indicate that HSJ-0017 is a potent dual SOD/CAT mimic.

In vivo antitumor effects of HSJ-0017

The antitumor effects of HSJ-0017 were investigated in H22 and S180 tumor-bearing mice. Results are presented in Table 1, Table 2, Figure 5, and Figure 6, respectively. Delayed tumor growth was observed in tumor-bearing mice treated with HSJ-0017 alone (group 2, Table 1 and Figure 6b). Compared with the vehicle control group (group 1), the tumor volume of the S180 tumor-bearing mice treated with HSJ-0017 shrank significantly ($P < 0.05$, Figure 6b), while that of H22 tumor-bearing mice treated with HSJ-0017 had no statistical difference when compared with group 1 ($P > 0.05$, Table 1). The tumor inhibition rate of HSJ-0017 on S180 tumor-bearing mice was found to be 22.38% (Table 2). The results of body weights (Table 1 and Figure 6a), peripheral blood counts (Figure 5), and immune organ indexes (Table 2) show that HSJ-0017 was well tolerated at the dose of 3 mg/kg ($P > 0.05$ compared with group 1). These results reveal that HSJ-0017 is a potent antitumor agent with more selective antitumor activity against S180 tumor.

In vivo radioprotective effects of HSJ-0017

The radioprotective effects of HSJ-0017 were investigated in H22 tumor-bearing mice. Results are presented in Table 1 and Figure 5, respectively. A single TBI of 7.0 Gy significantly reduced the tumor size of H22 tumor-bearing mice ($P < 0.01$ compared with group 1, Table 1) with a tumor inhibition rate of 28.83%. But TBI induced significant bone marrow suppression. As shown in Table 1 and Figure 5, compared with group 1, the body weight and peripheral blood counts of mice treated with TBI (group 3) decreased significantly ($P < 0.01$). Among them, WBC counts of mice sharply decreased three days after TBI. H22 tumor-bearing mice in groups 4–6 were given 3 mg/kg HSJ-0017 2 h before, 2 h after, or immediately after TBI. The body weight and peripheral blood counts of mice in groups 4–6 were significantly higher than those of mice in group 3 ($P < 0.05$ or $P < 0.01$, Table 1 and Figure 5). However, peripheral blood counts of mice in groups 4–6 were still considerably lower than those of mice in group 1 ($P < 0.05$ or $P < 0.01$, Figure 5) 10 days post irradiation. The tumor inhibition rate of group 5 was significantly higher than that of group 3, while that of group 6 was significantly lower than that of group 3. No significant difference in tumor inhibition rate was observed between group 3 and group 4. These results indicate that HSJ-0017 can attenuate TBI-induced bone marrow suppression and enhance the tumor killing activity of TBI. However, HSJ-0017 may counteract the antitumor effects of TBI when it was given simultaneously with TBI.

In vivo chemoprotective effects of HSJ-0017

The chemoprotective effects of HSJ-0017 were investigated in S180 tumor-bearing mice. Results are presented in Table 2 and Figure 6, respectively. CB administration resulted in a

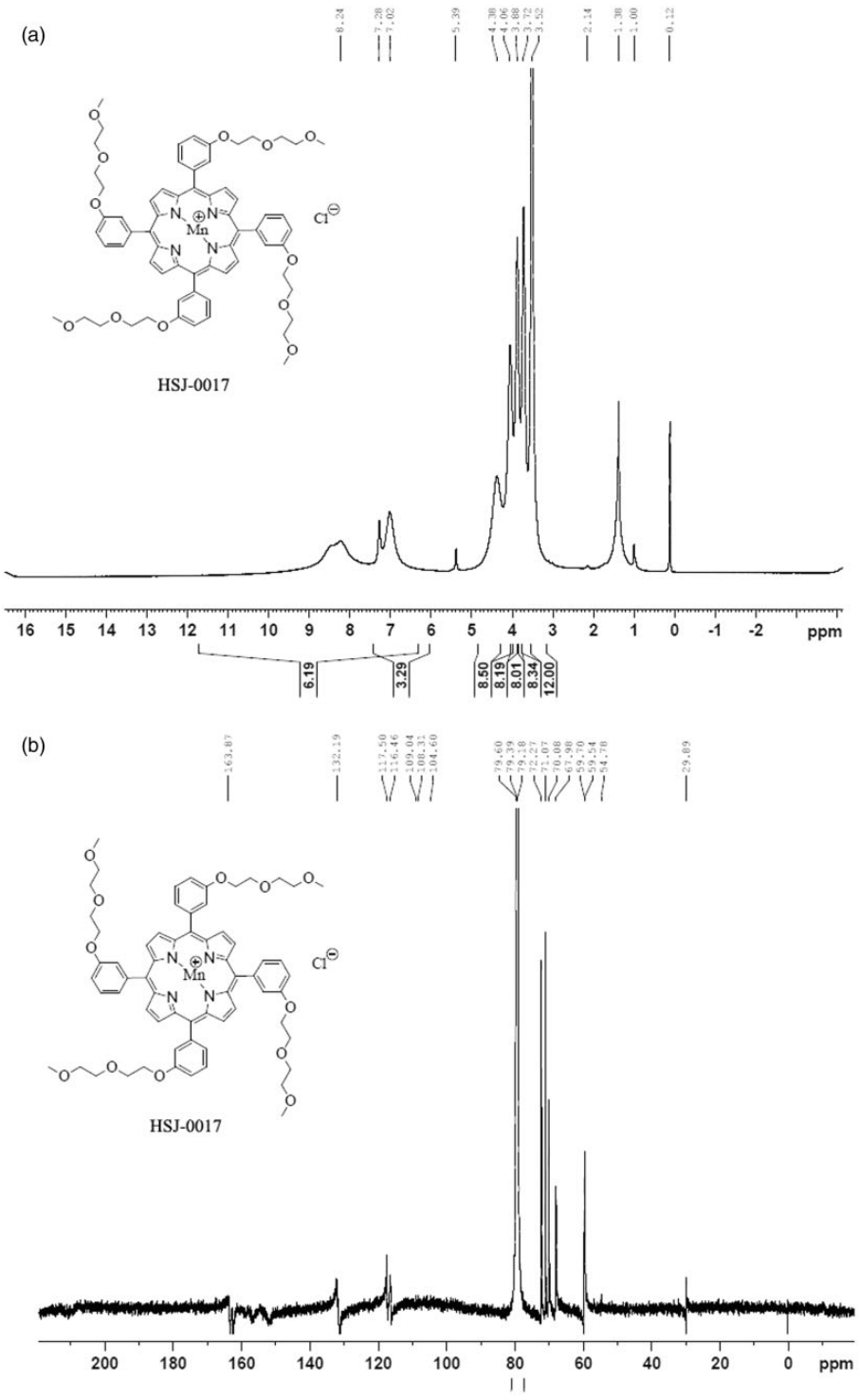

Figure 3 ^{1}H NMR (a) and ^{13}C NMR (b) spectra of HSJ-0017

tumor inhibition rate of 21.17% (group 3, Table 3 and Figure 6b). Compared with group 1, the body weights and immune organ indexes of S180 tumor-bearing mice treated with CB decreased significantly ($P < 0.01$, Table 2 and Figure 6a). S180 tumor-bearing mice in group 4 to group 6 were given 3 mg/kg HSJ-0017 2 h before, 8 h after or simultaneously with CB injection. The tumor inhibition rates of group 4 to group 6 were found to be 51.17%, 46.88%, and 59.13%, respectively. Compared with group 3, HSJ-0017 pre-, post- and co-administration significantly increased the tumor-inhibitory effect of CB ($P < 0.01$, Table 2). As shown in Table 2 and Figure 6a, the body weights and immune organ indexes of mice in group 4 to group 6 were significantly higher than those of mice in group 3 ($P < 0.05$ or

$P < 0.01$). Ten days after treatment, body weights and immune organ indexes of mice treated with CB in combination with HSJ-0017 recovered to a control level, except those of mice in group 4 ($P < 0.01$ compared with group 1). These results suggest that HSJ-0017 can enhance the tumor killing activity of CB and reduce CB-induced immunosuppression, regardless of pre-, post- or co-administration.

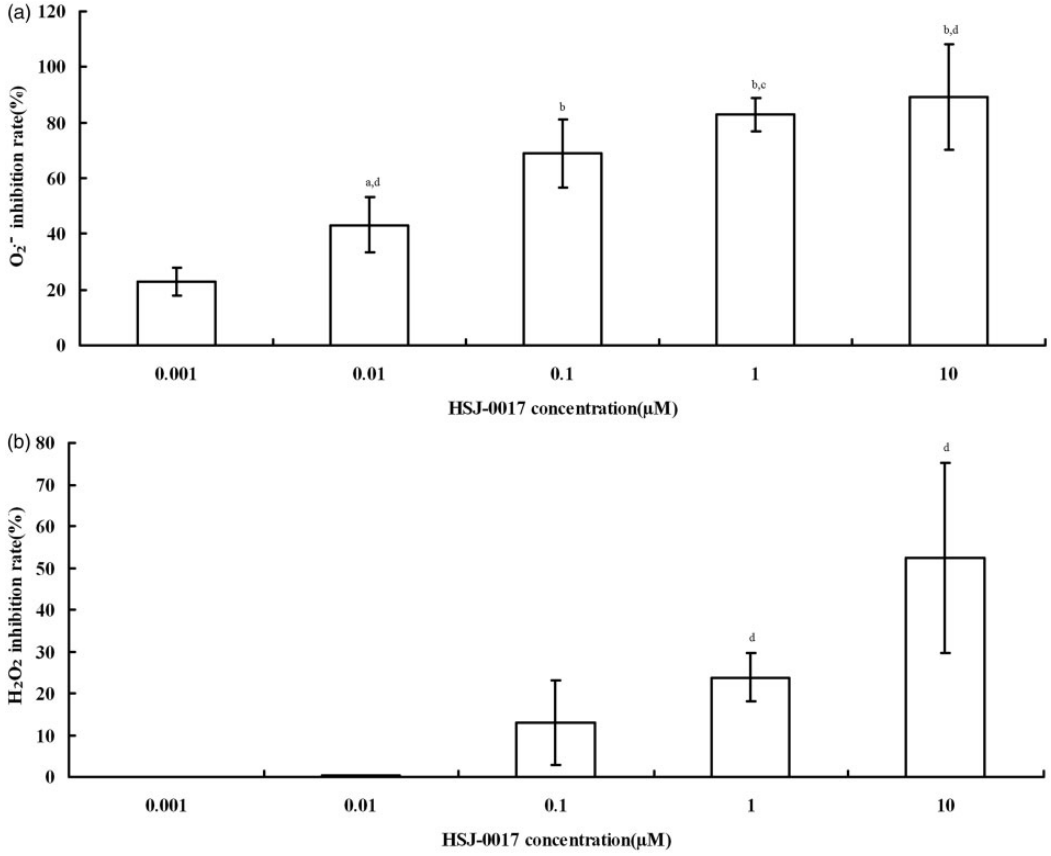

Figure 4 SOD and CAT mimic activities of HSJ-0017. SOD activity was measured in a reaction mixture containing 50 mmol/L sodium phosphate (pH 7.8), 250 μmol/L xanthine, 17.7 mU mL^{-1} xanthine oxidase, 2750 U mL^{-1} CAT, 10 μmol/L NBT, and various concentrations of HSJ-0017 (0.001, 0.01, 0.1, 1.0, and 10 μmol/L). Reduction of NBT was followed at 550 nm. The % inhibition of NBT reduction was calculated according to the following equation: % inhibition $= (A_0 - A_t/A_0) \times 100$; where A_0 was the absorbance of the control (without HSJ-0017) and A_t was the absorbance in the presence of HSJ-0017. CAT mimic activity was measured in a reaction mixture containing 50 mmol/L sodium phosphate (pH 7.0), 10 mmol/L H_2O_2, and various concentrations of HSJ-0017 (0.001, 0.01, 0.1, 1.0 and 10 μmol/L). Decomposition of H_2O_2 was monitored at 240 nm. The H_2O_2 scavenging activity of HSJ-0017 was calculated according to the following equation: H_2O_2 scavenging activity (%) $= (A_0 - A_t/A_0) \times 100$; where A_0 was the absorbance of the control and A_t was the absorbance in the presence of HSJ-0017. Values were expressed as mean ± SD. $^aP < 0.05$, $^bP < 0.01$ *versus* 0.001 μmol/L HSJ-0017; $^cP < 0.05$, $^dP < 0.01$ *versus* 0.1 μmol/L HSJ-0017

Table 1 Effects of HSJ-0017 and irradiation on body weight and tumor volume of H22 bearing mice (mean ± SD)

Groups	Body weight (g)		Tumor volume (mm^3)		Tumor inhibition rate (%)
	Pre-TBI	10 d post-TBI	Pre-TBI	10 d post-TBI	
Group 1	25.97 ± 2.80	32.96 ± 3.81	143.9 ± 35.0	745.0 ± 123.8	–
Group 2	25.34 ± 2.44	33.17 ± 3.54	141.8 ± 48.7	719.6 ± 205.3^b	3.88^b
Group 3	25.93 ± 2.12	27.35 ± 2.01^c	145.1 ± 39.4	572.9 ± 51.1^c	28.83
Group 4	24.96 ± 1.14	31.14 ± 2.16^b	140.9 ± 62.9	530.4 ± 37.6^{a,c}	35.20
Group 5	25.30 ± 0.82	32.31 ± 1.14^b	142.0 ± 26.2	425.7 ± 63.7^{b,c}	53.80^b
Group 6	25.17 ± 1.93	29.72 ± 2.39^a	141.3 ± 50.6	658.0 ± 71.2^{a,c}	14.04^b

Group 1 received NS containing 1% DMF, group 2 received 3.0 mg/kg HSJ-0017, group 3 received 7.0 Gy TBI, group 4 received 3.0 mg/kg HSJ-0017 followed 2 h later by 7.0 Gy TBI, group 5 received 7.0 Gy TBI followed 2 h later by 3.0 mg/kg HSJ-0017 and group 6 received 3.0 mg/kg HSJ-0017 immediately after 7.0 Gy TBI. Tumor inhibitory rate (%) = (1 − [ending average tumor volume of treatment group − starting average tumor volume of treatment group]/[ending average tumor volume of vehicle control group − starting average tumor volume of vehicle control group]) × 100%. $n = 10$.
$^aP < 0.05$ *versus* group 3.
$^bP < 0.01$ *versus* group 3.
$^cP < 0.01$ *versus* group 1.

Table 2 Organ indexes of S180-bearing mice and tumor inhibition rate of different groups (mean ± SD)

Groups	Thymus index (%)	Spleen index (%)	Tumor inhibition rate (%)
Group 1	0.23 ± 0.09	0.67 ± 0.15	–
Group 2	0.24 ± 0.08[b]	0.79 ± 0.14[b]	22.38
Group 3	0.07 ± 0.16[c]	0.30 ± 0.15[c]	21.17
Group 4	0.16 ± 0.03[a,c]	0.72 ± 0.07[b]	51.17[b]
Group 5	0.21 ± 0.08[b]	0.69 ± 0.14[b]	46.88[b]
Group 6	0.20 ± 0.16[b]	0.62 ± 0.03[b]	59.13[b]

Group 1 received NS containing 1% DMF, group 2 received 3.0 mg/kg HSJ-0017, group 3 received 30 mg/kg carboplatin, group 4 received 3.0 mg/kg HSJ-0017 followed 2 h later by 30 mg/kg carboplatin, group 5 received 30 mg/kg carboplatin followed 8 h later by 3.0 mg/kg HSJ-0017, and group 6 received 30 mg/kg carboplatin concurrent with 3.0 mg/kg HSJ-0017. HSJ-0017 and carboplatin were given by intravenous injection. Tumor inhibitory rate (%) was calculated using equation given in Table 1. $n = 10$.
[a]$P < 0.05$ *versus* group 3.
[b]$P < 0.01$ *versus* group 3.
[c]$P < 0.01$ *versus* group 1.

In vivo anti-inflammatory effects of HSJ-0017

The subplantar injection of histamine into the hind paw of Wistar rats evoked a significant paw swelling with a maximal rate detected at 6 h after histamine injection and thereafter declined at the end of the experiment. Figure 7 shows the time courses of the anti-inflammatory effects of dexamethasone and HSJ-0017 in histamine-induced paw edema model in rats. Compared with group 1 (vehicle control), dexamethasone at a dose of 1 mg/kg significantly reduced paw edema induced by histamine ($P < 0.01$). Despite a trend towards reduced paw swelling, HSJ-0017 at a dose of 0.3 mg/kg did not exhibit therapeutic anti-inflammatory effects ($P > 0.05$ compared with group 1), whereas at doses of 1.0 and 3.0 mg/kg, HSJ-0017 exhibited significant anti-inflammatory effects ($P < 0.05$ or $P < 0.01$ compared with group 1). No significant differences were observed between the dexamethasone treated group and the high dose HSJ-0017-treated group with respect to the percent change in edema volume (%) at all selected time points except at 6 h after histamine

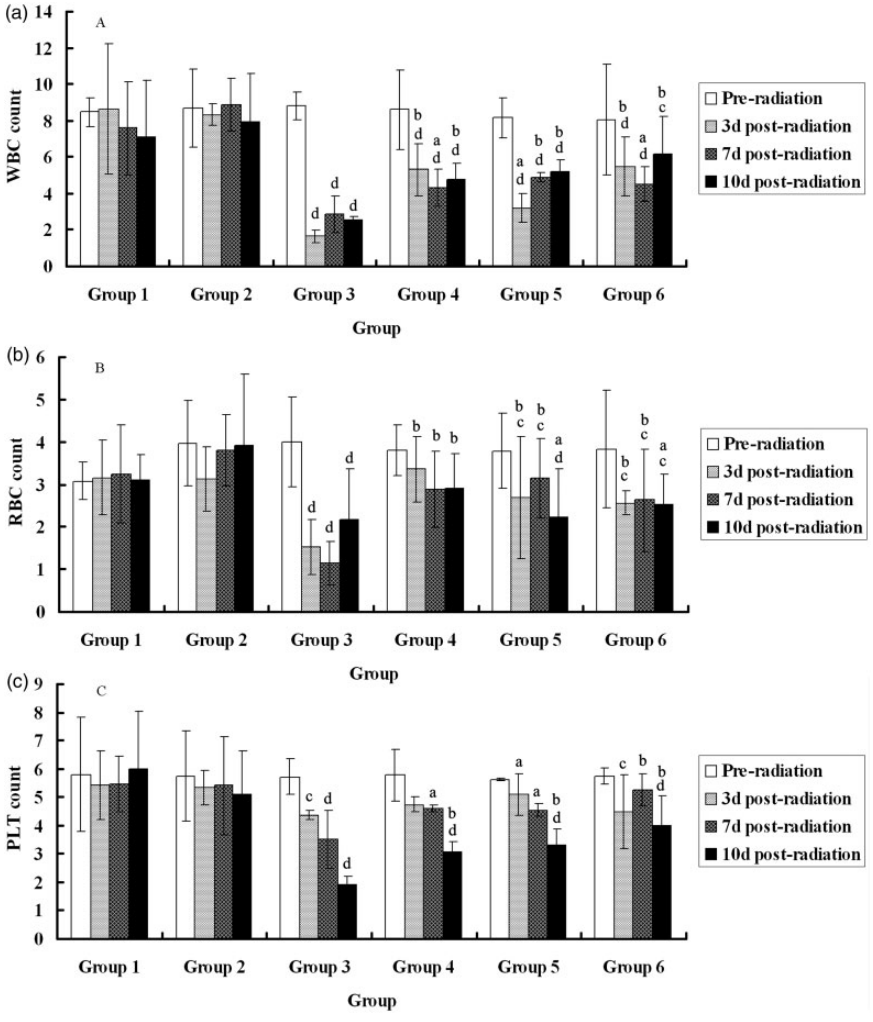

Figure 5 Effects of HSJ-0017 and irradiation on peripheral blood counts of H22 tumor-bearing mice. Group 1 received NS containing 1% DMF, group 2 received 3.0 mg/kg HSJ-0017, group 3 received 7.0 Gy TBI, group 4 received 3.0 mg/kg HSJ-0017 followed 2 h later by 7.0 Gy TBI, group 5 received 7.0 Gy TBI followed 2 h later by 3.0 mg/kg HSJ-0017, and group 6 received 3.0 mg/kg HSJ-0017 immediately after 7.0 Gy TBI. HSJ-0017 was given by intravenous injection. WBC: white blood cell ($\times 10^9$/mL), RBC: red blood cell ($\times 10^{12}$/mL), PLT: platelet ($\times 10^{12}$/mL). Values were expressed as mean ± SD. [a]$P < 0.05$, [b]$P < 0.01$ *versus* group 3; [c]$P < 0.05$, [d]$P < 0.01$ *versus* group 1

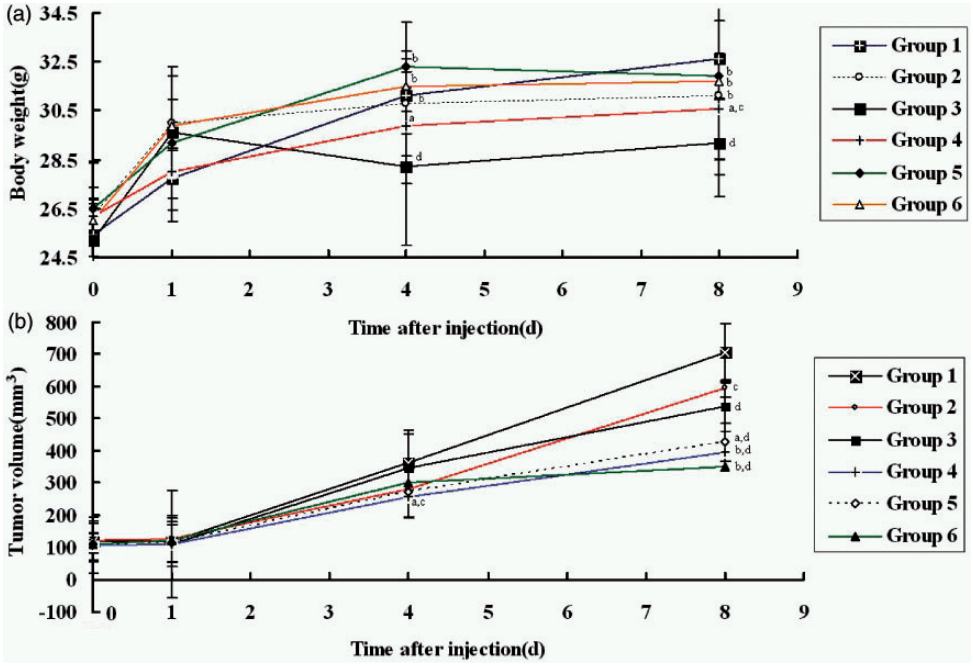

Figure 6 Effects of HSJ-0017 and carboplatin on body weight and tumor volume of S180 tumor-bearing mice. Group 1 received NS containing 1% DMF, group 2 received 3.0 mg/kg HSJ-0017, group 3 received 30 mg/kg carboplatin, group 4 received 3.0 mg/kg HSJ-0017 followed 2 h later by 30 mg/kg carboplatin, group 5 received 30 mg/kg carboplatin followed 8 h later by 3.0 mg/kg HSJ-0017, and group 6 received 30 mg/kg carboplatin concurrent with 3.0 mg/kg HSJ-0017. HSJ-0017 and carboplatin were given by intravenous injection. Tumor volume was calculated using the equation: $V = ab^2/2$, where a is the largest superficial diameter and b is the smallest superficial diameter. Values were expressed as mean ± SD. $^{a}P < 0.05$, $^{b}P < 0.01$ *versus* group 3; $^{c}P < 0.05$, $^{d}P < 0.01$ *versus* group 1

Table 3 Effects of HSJ-0017 on serum and hepatic biochemical indices in rats with CCl_4-induced hepatic damage (mean ± SD)

Groups	ALT (IU/L)	AST (IU/L)	ALP (IU/L)	LDH (IU/L)	GGT (IU/L)	SOD (U/mg protein)	CAT (U/mg protein)	GPx (U/mg zprotein)
Group 1	32.7 ± 4.1	178.4 ± 12.7	248.5 ± 27.3	105.8 ± 19.4	1.4 ± 0.8	149.0 ± 16.3	32.2 ± 8.5	29.1 ± 1.7
Group 2	210.3 ± 29.2^{d}	493.2 ± 34.4^{d}	561.1 ± 83.0^{d}	431.5 ± 96.8^{d}	8.7 ± 1.1^{d}	52.8 ± 5.1^{d}	14.4 ± 2.9^{c}	12.6 ± 0.1^{d}
Group 3	189.0 ± 10.9^{d}	552.7 ± 72.1^{d}	558.2 ± 67.5^{d}	257.0 ± 12.7^{a,c}	4.1 ± 0.5^{a,c}	109.4 ± 30.8^{a,c}	19.6 ± 1.2^{c}	15.9 ± 1.4^{d}
Group 4	141.6 ± 16.3^{a,d}	313.8 ± 44.6^{a,c}	471.9 ± 39.2^{a,d}	206.4 ± 41.0^{a,c}	1.3 ± 0.3^{b}	124.9 ± 8.2^{b}	23.0 ± 1.8^{a}	19.2 ± 3.9^{a,c}
Group 5	136.9 ± 11.5^{b,d}	165.1 ± 19.0^{b}	294.6 ± 51.7^{b}	120.2 ± 34.1^{b}	1.1 ± 0.5^{b}	161.3 ± 12.7^{b}	30.7 ± 2.1^{b}	24.7 ± 2.6^{b}

Group 1 received olive oil only, group 2 received CCl_4 combined with NS containing 1% DMF (model control, group 2), groups 3–5 received CCl_4 combined with different doses of HSJ-0017 (0.3, 1.0 and 3.0 mg/kg). Both vehicles and HSJ-0017 were given once daily intravenously for 28 consecutive days. SOD activity was assayed in a reaction mixture consisted of 0.8 mL of 50 mmol/L glycine buffer (pH 10.4) 0.02 mL of 20 mg/mL solution of (–) epinephrine and 0.2 mL PMS. CAT activity was assayed in a reaction mixture (3.0 mL) consisted of 0.05 mol/L sodium phosphate buffer (pH 7.0) 0.019 mol/L H_2O_2 and 0.05 mL PMS. Decomposition of H_2O_2 was monitored at 240 nm at 25°C. GPx activity was assayed in a reaction mixture (2.0 mL) consisted of 0.2 mmol/L H_2O_2, 1 mmol/L glutathione, 1.43 mmol/L NADPH, 1 mmol/L sodium azide, 0.1 mol/L sodium phosphate buffer (pH 7.0), 1.4 unit of glutathione reductase, and 0.1 mL PMS. $N = 10$.
$^{a}P < 0.05$ *versus* group 2.
$^{b}P < 0.01$ *versus* group 2.
$^{c}P < 0.05$ *versus* group 1.
$^{d}P < 0.01$ *versus* group 1.

injection. These results suggest that HSJ-0017 possesses significant anti-inflammatory activity.

In vivo hepatoprotective effects of HSJ-0017

Serum levels of certain marker enzymes, including ALT, AST, ALP, LDH, and GGT are highly susceptible to hepatotoxins. They serve as markers of hepatic damage. The activities of hepatic SOD, CAT, and GPx were measured as indexes of tissue antioxidant status. As summarized in Table 3, serum levels of ALT, AST, ALP, LDH, and GGT enzymes in the model control group (group 2) were significantly higher than those in the normal control group ($P < 0.01$), which reflected the severity of hepatic injury. Treatment with HSJ-0017 at doses of 1.0 and 3.0 mg/kg significantly decreased the serum levels of ALT, AST, ALP,

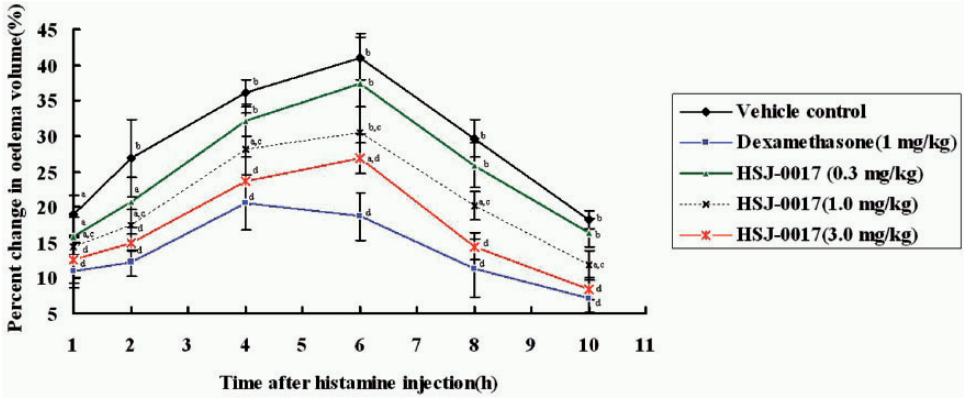

Figure 7 Anti-inflammatory effects of HSJ-0017 on histamine-induced paw edema in rats. Paw edema was induced by subplantar injection of 0.1 mL of 0.1% freshly prepared solution of histamine into the right hind paw of Wistar rats. HSJ-0017 and dexamethasone were given by intraperitoneal injection 1 h before eliciting paw edema. Percent change in edema volume was calculated according to the following equation: Percent change in edema volume (%) = $(V_t - V_0)/V_0 \times 100\%$, where V_0 (mL) was the average paw volume before injection and V_t (mL) was the average paw volume after injection

LDH, and GGT ($P < 0.05$ or $P < 0.01$ compared with group 2), whereas HSJ-0017 at a dose of 0.3 mg/kg only decreased serum levels of LDH and GGT ($P < 0.05$ compared with group 2).

Histological observations basically supported the results obtained from serum enzyme assays. There were no obvious histological changes in the livers of normal rats (Figure 8a). On the contrary, liver sections from rats treated with CCl_4 only showed severe hepatocellular necrosis, with extensive cellular swelling and fatty change (Figure 8b). Treatment with HSJ-0017 remarkably reversed the histological changes caused by CCl_4. Liver sections from rats treated with 0.3 mg/kg HSJ-0017 showed mild hepatocellular necrosis and swelling, as well as fatty change (Figure 8c). Liver sections from rats treated with 1.0 mg/kg HSJ-0017 showed moderate injury exhibiting cytoplasmic relaxation and vacuolization (Figure 8d). Histopathological observations of the liver of rats treated with 3.0 mg/kg HSJ-0017 showed normal hepatic architecture, almost comparable to the normal control (Figure 8e).

Effects of HSJ-0017 on the activity of hepatic SOD, CAT, and GPx were shown in Table 3. The activities of these enzymes were significantly depleted in the model control group as compared to the normal control group. HSJ-0017 at doses of 0.3, 1.0, and 3.0 mg/kg significantly increased the activity of these enzymes in a dose-dependent manner ($P < 0.05$ or $P < 0.01$ compared with group 2). Treatment with 3.0 mg/kg HSJ-0017 dramatically restored the activities of hepatic antioxidant enzymes to normal. These results suggest the possibility that HSJ-0017 provides protection against oxidative stress-induced hepatic injury.

Discussion

HSJ-0017 is a novel lipophilic Mn porphyrin. It is designed with a redox-active Mn(III) center, which can catalyze the dismutation reaction of O_2^- by a mechanism similar to that of SOD. Four diethylene glycol monomethyl ether chains on *meso*-phenyl rings are designed to facilitate the distribution of HSJ-0017 within tissues and to prevent molecule-overlapping and drug–DNA interactions so as to reduce the toxicity of HSJ-0017.[16,35] Our previous studies have proven that HSJ-0017 has a wide tissue distribution with low toxicity.[17,18]

In the present study, we investigated the *in vitro* enzyme-mimic activity and *in vivo* therapeutic potential of HSJ-0017. Our results suggested that HSJ-0017 is active in scavenging O_2^- and H_2O_2 at micromolar concentrations. Meanwhile, *in vivo* studies in mice and rats showed that HSJ-0017 possesses significant anti-inflammatory and hepatoprotective effects, and can enhance the antitumor effects and attenuate the toxic effects of radiotherapy and chemotherapy. For *in vivo* antitumor effects, we found that HSJ-0017 is effective against S180 tumor xenografts but less effective against H22 tumor xenografts. Furthermore, we found for the first time, that the beneficial effects of HSJ-0017 on antitumor activity and toxicity of radiotherapy may be affected by the timing of drug administration. The therapeutic potential of HSJ-0017 against free radical related central nervous system diseases was not investigated in the present study in view of the fact that HSJ-0017 displays poor blood-brain barrier permeability.[17]

O_2^- and H_2O_2 have been a subject of intense interest owing to their increased dominance *in vivo* in different disease conditions. Although O_2^- and H_2O_2 are far less active than ·OH, they can generate ·OH in the biological system, and subsequently induce extensive oxidative stress.[36] In the present study, we found that HSJ-0017 exhibits high O_2^- scavenging activity, as shown by the IC_{50} value. Although the assay methods differed, the SOD mimic activity of HSJ-0017 was higher than that of AEOL11207, a lipophilic Mn-porphyrin undergoing preclinical evaluation (HSJ-0017 is about 20-fold less active than Cu/Zn SOD, whereas AEOL11207 is 123-fold less active[37]). Given that both HSJ-0017 and AEOL11207 are lipophilic, uncharged Mn-porphyrins, it can be speculated that the differences in SOD activity may be related to the substituents at the meso-positions of the porphyrin ring. In the present study, we also found that HSJ-0017 has significant H_2O_2 scavenging activity, despite lacking significant activity at low concentrations. Similar results have also been reported for other

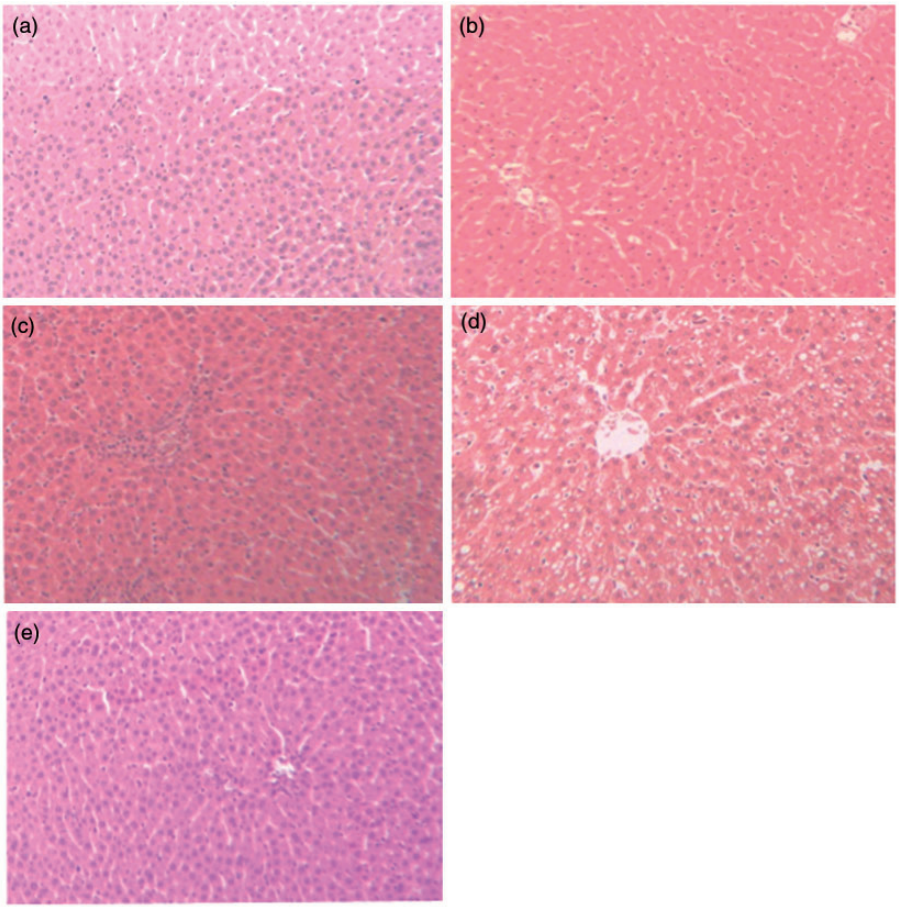

Figure 8 Histological features of liver sections stained with H-E after CCl_4 treatment. Typical images were chosen from the different groups (100 × magnification). a: normal control group, showing normal hepatic architecture; b: vehicle-treated model control, showing severe hepatocellular necrosis with extensive cellular swelling and fatty change; c: HSJ-0017 0.3 mg/kg + CCl_4 group, showing mild hepatocellular necrosis, swelling, and fatty change; d: HSJ-0017 1.0 mg/kg + CCl_4 group, showing moderate injury exhibiting cytoplasmic relaxation and vacuolization; e: HSJ-0017 3.0 mg/kg + CCl_4 group, showing normal hepatic architecture

Mn-porphyrins which show high SOD mimic activity and low CAT mimic activity.[25] The CAT mimic activity of HSJ-0017 could be attributed to its conjugated ring system (Figure 1), which has a structure similar to the heme prosthetic group of endogenous CAT.[38]

The fact that free radicals participate in tumor initiation by promoting DNA damage has been long accepted, thus natural antioxidants have been widely used in cancer prevention. Several Mn porphyrin-based SOD mimics, in particular lipophilic analogues, have been proven effective in treating specific types of cancer.[39,40] The relationship between free radicals and carcinogenesis is increasingly well documented, with numerous reports of cancer cells showing higher levels of free radicals compared with normal cells.[41] There are multiple lines of evidence in the literature to support the hypothesis that free radicals are capable of promoting tumor vascular angiogenesis and antioxidants have antiangiogenic activity.[42] Based on the relationships among free radicals, inflammation and carcinogenesis,[43] the antitumor effect of HSJ-0017 is presumably ascribed to its antioxidant and anti-inflammatory properties. Nonetheless, the precise mechanism underlying the antitumor effect of Mn porphyrin-based SOD mimics still requires further investigation. HSJ-0017 was found to be less effective against H22 tumor xenografts. This result is in accordance with our *in vitro* antitumor assays, which shows that H22 hepatoma cells are insensitive to HSJ-0017 (unpublished data). Thus, the low inhibitory effect of HSJ-0017 against H22 tumor may be at least in part because H22 hepatoma cells are lack of response to HSJ-0017. However, further dose escalating experiments and long-term experiments are still needed.

Free radicals are responsible for radiotherapy- and chemotherapy-induced normal tissue damages, due to their non-selective nature.[1] However, in the meantime, excessive free radicals could help kill cancer cells by blocking key steps in the cell cycle.[44] Despite comprehensive review articles concluding that antioxidants do not undermine the effectiveness of cytotoxic therapies, the use of antioxidants during radiotherapy- and chemotherapy remains controversial. Based on the double-edged sword role of free radicals in cancer treatment, we hypothesized that when HSJ-0017 is delivered simultaneously with radiotherapy or chemotherapy, it may counteract the antitumor effects of conventional treatments. To rule out the possibility that this counteractive effect may be concealed by the

antitumor effect of HSJ-0017, a tumor cell line that is insensitive to HSJ-0017 (H22 hepatoma cell) was used in the present study. Our results obtained from H22 tumor-bearing mice preliminarily support this hypothesis. Similar results have been recently reported in the literature.[19,20] Results obtained from S180 tumor-bearing mice indicated that HSJ-0017 can enhance the tumor killing activity of CB, regardless of pre-, post- or co-administration. One possible reason for this disagreement is that the mechanism of action of CB may be independent of free radical intermediates or free radical generation.[45] It could also be explained by the antitumor effect of HSJ-0017.

CCl_4 is known to exert its toxicity through its metabolites, including the free radicals.[46] Therefore, in the present study, *in vivo* antioxidant activity was measured as part of hepatoprotective activity assays by examining the activity levels of various hepatic antioxidant enzymes. Results showed that HSJ-0017 can significantly increase the activity levels of hepatic SOD, CAT, and GPx. Thus, the hepatoprotective effect of HSJ-0017 may be at least in part attributed to its beneficial effects on hepatic antioxidant enzymes.

In summary, the results of the present study demonstrate that HSJ-0017 is a potent dual SOD/CAT mimic. It exhibits antioxidant, antitumor, anti-inflammatory, and hepatoprotective effects *in vivo*, and can enhance the antitumor effects of radiotherapy and chemotherapy, and reduce the negative side effects of radiotherapy and chemotherapy. However, HSJ-0017 may counteract the antitumor effects of radiotherapy when it is administered simultaneously with radiotherapy.

Author contributions: B-qL and F-sW designed the research; QY and S-hF prepared and identified the test compound. XD, NL, J-yG, X-cG, and S-jW performed the *in vitro* and *in vivo* studies; X-D, J-yG and X-cG analyzed the results and wrote the paper.

ACKNOWLEDGMENTS

The authors would like to thank Dr Xian-Jun Qu for his valuable assistance in the preparation of the manuscript for this article. This work was supported by Natural Science Foundation of Shandong Province (No. 2009ZRB019AO) and National Major Scientific and Technological Special Project for ''Significant New Drugs Development'' during the Twelfth Five-year Plan Period (No. 2013ZX09J13102-03C).

REFERENCES

1. Moss RW. Do antioxidants interfere with radiation therapy for cancer? *Integr Cancer Ther* 2007;**6**:281–92
2. Salvemini D, Doyle TM, Cuzzocrea S. Superoxide, peroxynitrite and oxidative/nitrative stress in inflammation. *Biochem Soc Trans* 2006;**34**:965–70
3. Zweier JL, Talukder MA. The role of oxidants and free radicals in reperfusion injury. *Cardiovasc Res* 2006;**70**:181–90
4. Ahn MR, Kunimasa K, Kumazawa S, Nakayama T, Kaji K, Uto Y, Hori H, Nagasawa H, Ohta T. Correlation between antiangiogenic activity and antioxidant activity of various components from propolis. *Mol Nutr Food Res* 2009;**53**:643–51
5. Simůnek T, Stérba M, Popelová O, Adamcová M, Hrdina R, Gersl V. Anthracycline-induced cardiotoxicity: overview of studies examining the roles of oxidative stress and free cellular iron. *Pharmacol Rep* 2009;**61**:154–71
6. Husain K, Whitworth C, Hazelrigg S, Rybak L. Carboplatin-induced oxidative injury in rat inferior colliculus. *Int J Toxicol* 2003;**22**:335–42
7. Bouayed J, Bohn T. Exogenous antioxidants-double-edged swords in cellular redox state: health beneficial effects at physiologic doses versus deleterious effects at high doses. *Oxid Med Cell Longev* 2010;**3**:228–37
8. Iranzo O. Manganese complexes displaying superoxide dismutase activity: a balance between different factors. *Bioorg Chem* 2011;**39**:73–87
9. Angelova M, Dolashka-Angelova P, Ivanova E, Serkedjieva J, Slokoska L, Pashova S, Toshkova R, Vassilev S, Simeonov I, Hartmann HJ, Stoeva S, Weser U, Voelter W. A novel glycosylated Cu/Zn-containing superoxide dismutase: production and potential therapeutic effect. *Microbiology* 2001;**147**:1641–50
10. Ishihara T, Tanaka K, Tasaka Y, Namba T, Suzuki J, Ishihara T, Okamoto S, Hibi T, Takenaga M, Igarashi R, Sato K, Mizushima Y, Mizushima T. Therapeutic effect of lecithinized superoxide dismutase against colitis. *J Pharmacol Exp Ther* 2009;**328**:152–64
11. Hayakawa N, Asayama S, Noda Y, Shimizu T, Kawakami H. Pharmaceutical effect of manganese porphyrins on manganese superoxide dismutase deficient mice. *Mol Pharm* 2012;**9**:2956–59
12. Lubos E, Loscalzo J, Handy DE. Glutathione peroxidase-1 in health and disease: from molecular mechanisms to therapeutic opportunities. *Antioxid Redox Signal* 2011;**15**:1957–97
13. The Alpha-Tocopherol, Beta Carotene Cancer Prevention Study Group. The effect of vitamin E and beta carotene on the incidence of lung cancer and other cancers in male smokers. *N Engl J Med* 1994;**330**:1029–35
14. Rosenthal RA, Huffman KD, Fisette LW, Damphousse CA, Callaway WB, Malfroy B, Doctrow SR. Orally available Mn-porphyrins with superoxide dismutase and catalase activities. *Biol Inorg Chem* 2009;**14**:979–91
15. Oury TD, Thakker K, Menache M, Chang LY, Crapo JD, Day BJ. Attenuation of bleomycin-induced pulmonary fibrosis by a catalytic antioxidant metalloporphyrin. *Am J Respir Cell Mol Biol* 2001;**25**:164–9
16. Rajic Z, Tovmasyan A, Spasojevic I, Sheng H, Lu M, Li AM, Gralla EB, Warner DS, Benov L, Batinic-Haberle I. A new SOD mimic, Mn(III) ortho N-butoxyethylpyridylporphyrin, combines superb potency and lipophilicity with low toxicity. *Free Radic Biol Med* 2012;**52**:1828–34
17. Li BQ, Fang SH, Dong X, Li N, Gao JY, Yang GQ, Gong XC, Wang SJ, Wang FS. Pharmacokinetics, tissue distribution and excretion of manganese (III) meso-tetra [3-(2-(2-methoxy)-ethoxy) ethoxy] phenyl porphyrin chloride, a novel superoxide dismutase mimic, in Wistar rats. *Eur J Drug Metab Pharmacokinet* 2013;**38**:245–53
18. Li BQ, Dong X, Yang GQ, Li N, Gao JY, Fang SH, Gong XC, Wang SJ, Wang FS. A novel superoxide dismutase mimic, HSJ-0017, reduces radiation-induced and chemotherapy-induced damage. *Lat Am J Pharm* 2013;**32**:257–62
19. Wambi C, Sanzari J, Wan XS, Nuth M, Davis J, Ko YH, Sayers CM, Baran M, Ware JH, Kennedy AR. Dietary antioxidants protect hematopoietic cells and improve animal survival after total-body irradiation. *Radiat Res* 2008;**169**:384–96
20. Brown SL, Kolozsvary A, Liu J, Jenrow KA, Ryu S, Kim JH. Antioxidant diet supplementation starting 24 hours after exposure reduces radiation lethality. *Radiat Res* 2010;**173**:462–8
21. Liu CS, Cheng Y, Hu JF, Zhang W, Chen NH, Zhang JT. Comparison of antioxidant activities between salvianolic acid B and Ginkgo biloba extract (EGb 761). *Acta Pharmacol Sin* 2006;**27**:1137–45
22. Berkó G, Schneider I. A method for quantitative determination of nitroblue tetrazolium. *Z Med Lab Diagn* 1983;**24**:327–31
23. Giblin GM, Box PC, Campbell IB, Hancock AP, Roomans S, Mills GI, Molloy C, Tranter GE, Walker AL, Doctrow SR, Huffman K, Malfroy B. 6,6′-Bis(2-hydroxyphenyl)-2,2′-bipyridine manganese(III) complexes: a novel series of superoxide dismutase and catalase mimetics. *Bioorg Med Chem Lett* 2001;**11**:1367–70
24. Beers RF Jr, Sizer IW. A spectrophotometric method for measuring the breakdown of hydrogen peroxide by catalase. *J Biol Chem* 1952;**195**:133–40

25. Rosenthal RA, Huffman KD, Fisette LW, Damphousse CA, Callaway WB, Malfroy B, Doctrow SR. Orally available Mn porphyrins with superoxide dismutase and catalase activities. *J Biol Inorg Chem* 2009;**14**:979–91
26. Gao YS, Zhu YY, Gao YH, Li J, Qin QL, Qiu YF, Tong RT. Comparison of antitumor effects and pharmacokinetics of carboplatin administered intratumorally and intravenously in mice with tumor. *Chin Pharmacol Bull* 1999;**15**:160–63
27. Hira A, Dey SK, Howlader MS, Ahmed A, Hossain H, Jahan IA. Anti-inflammatory and antioxidant activities of ethanolic extract of aerial parts of Vernonia patula (Dryand.) Merr. *Asian Pac J Trop Biomed* 2013;10): 798–805
28. Farshid AA, Tamaddonfard E, Morvaridi A. Effects of histidine and dexamethasone on the local inflammation induced by histamine in rats. *Vet Res Forum* 2011;**2**:31–6
29. Sikander M, Malik S, Parveen K, Ahmad M, Yadav D, Hafeez ZB, Bansal M. Hepatoprotective effect of Origanum vulgare in Wistar rats against carbon tetrachloride-induced hepatotoxicity. *Protoplasma* 2013;**250**:483–93
30. Mármol F, Sánchez J, López D, Martínez N, Xaus C, Peralta C, Roselló-Catafau J, Mitjavila MT, Puig-Parellada P. Role of oxidative stress and adenosine nucleotides in the liver of aging rats. *Physiol Res* 2010;**59**:553–60
31. Batinic-Haberle I, Rajic Z, Tovmasyan A, Reboucas JS, Ye X, Leong KW, Dewhirst MW, Vujaskovic Z, Benov L, Spasojevic I. Diverse functions of cationic Mn(III) N-substituted pyridylporphyrins, recognized as SOD mimics. *Free Radic Biol Med* 2011;**51**:1035–53
32. Moore DE, Wang J. Electron-transfer mechanisms in photosensitization by the anti-inflammatory drug benzydamine. *J Photochem Photobiol B* 1998;**43**:175–80
33. Trova MP, Gauuan PJ, Pechulis AD, Bubb SM, Bocckino SB, Crapo JD, Day BJ. Superoxide dismutase mimetics. Part 2: synthesis and structure-activity relationship of glyoxylate- and glyoxamide-derived metalloporphyrins. *Bioorg Med Chem* 2003;**11**:2695–707
34. Chen CN, Pan SM. Assay of superoxide dismutase activity by combining electrophoresis and densitometry. *Bot Bull Acad Sin* 1996;**37**:107–11
35. Kachadourian R, Menzeleev R, Agha B, Bocckino SB, Day BJ. High-performance liquid chromatography with spectrophotometric and electrochemical detection of a series of manganese(III) cationic porphyrins. *J Chromatogr B Analyt Technol Biomed Life Sci* 2002;**767**:61–7
36. Devasagayam TP, Tilak JC, Boloor KK, Sane KS, Ghaskadbi SS, Lele RD. Free radicals and antioxidants in human health: current status and future prospects. *J Assoc Physicians India* 2004;**52**:794–804
37. Liang LP, Huang J, Fulton R, Day BJ, Patel M. An orally active catalytic metalloporphyrin protects against 1-methyl-4-phenyl-1,2,3,6-tetrahydropyridine neurotoxicity in vivo. *J Neurosci* 2007;**27**:4326–33
38. Cuzzocrea S, Riley DP, Caputi AP, Salvemini D. Antioxidant therapy: a new pharmacological approach in shock, inflammation, and ischemia/reperfusion injury. *Pharmacol Rev* 2001;**53**:135–59
39. Moeller BJ, Batinic-Haberle I, Spasojevic I, Rabbani ZN, Anscher MS, Vujaskovic Z, Dewhirst MW. A manganese porphyrin superoxide dismutase mimetic enhances tumor radioresponsiveness. *Int J Radiat Oncol Biol Phys* 2005;**63**:545–52
40. Keir ST, Dewhirst MW, Kirkpatrick JP, Bigner DD, Batinic-Haberle I. Cellular redox modulator, ortho Mn(III) meso-tetrakis(N-n-Hexylpyridinium-2-yl)porphyrin, MnTnHex-2-PyP5+ in the treatment of brain tumors. *Anticancer Agents Med Chem* 2011;**11**:202–12
41. Sainz RM, Lombo F, Mayo JC. Radical decisions in cancer: redox control of cell growth and death. *Cancers* 2012;**4**:442–74
42. Dewhirst MW, Cao Y, Moeller B. Cycling hypoxia and free radicals regulate angiogenesis and radiotherapy response. *Nat Rev Cancer* 2008;**8**:425–37
43. Hussain SP, Hofseth LJ, Harris CC. Radical causes of cancer. *Nat Rev Cancer* 2003;**3**:276–85
44. Simone CB 2nd, Simone NL, Simone V, Simone CB. Antioxidants and other nutrients do not interfere with chemotherapy or radiation therapy and can increase kill and increase survival, part 1. *Altern Ther Health Med* 2007;**13**:22–8
45. Conklin KA. Cancer chemotherapy and antioxidants. *J Nutr* 2004;**134**:3201S–4S
46. Burk RF, Lane JM, Patel K. Relationship of oxygen and glutathione in protection against carbon tetrachloride-induced hepatic microsomal lipid peroxidation and covalent binding in the rat. Rationale for the use of hyperbaric oxygen to treat carbon tetrachloride ingestion. *J Clin Invest* 1984;**74**:1996–2001

(Received January 20, 2014, Accepted March 11, 2014)